

Cascade time-scales for energy and helicity in homogeneous, isotropic turbulence

Susan Kurien

*Center for Nonlinear Studies and Theoretical Division,
Los Alamos National Laboratory, Los Alamos, New Mexico 87545, U.S.A.*

Mark A. Taylor

*Computer and Computational Sciences Division,
Los Alamos National Laboratory, Los Alamos, New Mexico 87545, U.S.A.*

Takeshi Matsumoto

*Department of Physics, Kyoto University,
Kitashirakawa Oiwakecho Sakyo-ku, Kyoto 606-8502, Japan*

(Dated: February 9, 2020)

Abstract

We derive a time-scale τ_H for energy and helicity transfer in homogeneous, isotropic turbulence from the helical co-spectrum, using the arguments of Kraichnan (J. Fluid Mech. **47**, 525–535 (1971)). While the Kraichnan time-scale, τ_E , depends on in-plane shearing motions derived from reflection-symmetric velocity correlations, τ_H depends on out-of-plane shearing motions introduced by the presence of helicity. We show that in general τ_H may not be neglected even for rather low relative helicity. We postulate an inertial range joint cascade in which the dynamics are dominated by τ_E in the low wavenumbers with spectra scaling as $k^{-5/3}$; and by τ_H at larger wavenumbers with spectra scaling as $k^{-4/3}$. The commonly observed “bottleneck” in the energy spectrum might be explained by such a two-stage cascade. We derive a wavenumber k_h which is less than the Kolmogorov dissipation wavenumber, at which both energy and helicity cascades terminate due to dissipation effects. Data from direct numerical simulations are used to check our predictions.

PACS numbers: 47.27.Gs, 47.27.Jv, 47.27.Eq

Energy and helicity [1, 2] are the two known inviscid invariants of the Navier–Stokes equations. It was postulated in [3] that in isotropic flows with helicity, these quantities cascade together from large to small scales. This joint forward cascade of energy and helicity has been verified by direct numerical simulations, most recently at a resolution of 512^3 gridpoints [4]. Kraichnan [5] defined the shear time-scale τ_E for energy transfer, based solely on energy dynamics. Assuming that helicity dynamics are also controlled by τ_E , a $k^{-5/3}$ inertial range scaling was established for both energy and helicity spectra [3].

We recall the spectral formulation $\langle u_i(\mathbf{k})u_j^*(\mathbf{k}) \rangle$ of the two-point velocity correlation function in isotropic, homogeneous, statistically stationary turbulence. It may be decomposed into its index-symmetric and index-antisymmetric parts as

$$E_{ij}(\mathbf{k}) = \frac{1}{2} \left(\langle u_i(\mathbf{k})u_j^*(\mathbf{k}) \rangle + \langle u_j(\mathbf{k})u_i^*(\mathbf{k}) \rangle \right), \quad (1)$$

$$\tilde{E}_{ij}(\mathbf{k}) = \frac{1}{2} \left(\langle u_i(\mathbf{k})u_j^*(\mathbf{k}) \rangle - \langle u_j(\mathbf{k})u_i^*(\mathbf{k}) \rangle \right), \quad (2)$$

where i and j denote any of the components in a cartesian coordinate system. Eq. (1) when contracted with $\delta_{ij}/2$ and then averaged over $\hat{\mathbf{k}}$ gives the energy spectrum $E(k)$. Similarly, Eq. (2) when contracted with the curl operator $\hat{i}\varepsilon_{ijl}k_l$, where $\hat{i} = \sqrt{-1}$, and then averaged over $\hat{\mathbf{k}}$ gives the total helicity density $H(k) = 2k\tilde{E}(k)$. (Note that this relationship is distinct from the Schwartz-inequality $|H(k)| \leq 2kE(k)$). Here $E(k) = \sum_{|\mathbf{k}|=k} \frac{1}{2} |\tilde{\mathbf{u}}(\mathbf{k})|^2$ and $H(k) = \sum_{|\mathbf{k}|=k} \tilde{\mathbf{u}}(\mathbf{k}) \cdot \tilde{\boldsymbol{\omega}}(-\mathbf{k})$ where $\tilde{\mathbf{u}}(\mathbf{k})$ and $\tilde{\boldsymbol{\omega}}(\mathbf{k})$ are the fourier transforms of the velocity $\mathbf{u}(\mathbf{x})$ and the vorticity $\boldsymbol{\omega}(\mathbf{x}) = \nabla \times \mathbf{u}(\mathbf{x})$ respectively.

The time-scale for energy transfer, τ_E , corresponds to correlations of the type $E_{ij}(\mathbf{k})$ (Eq. (1)) which arise due to shearing motions in the plane of coordinates i, j and $\hat{\mathbf{k}}$. Such ‘in-plane’ shearing motions cannot give rise to correlations of the type $\tilde{E}_{ij}(\mathbf{k})$ (Eq. (2)) which relate orthogonal components i and j across the third mutually orthogonal direction $\hat{\mathbf{k}}$. For this we require ‘out-of-plane’ shearing motions, which are provided by the presence of helicity [6, 7]. We derive the time-scale, τ_H , associated with such an out-of-plane shear. The governing factor is the relative helicity $|H(k)|/(2kE(k))$ which will be shown to fall off linearly in wavenumber restoring parity as k becomes very large. Crucially, we will show that the ratio $\tau_E/\tau_H \sim (|H(k)|/(2kE(k)))^{1/2}$, which decays slower than the relative helicity. Therefore, the effect of τ_H cannot be neglected. We demonstrate the effect of this new timescale on energy and helicity spectra, and offer an interpretation of the ‘bottleneck’ effect observed in measured energy spectra. Finally, the new dynamics reveal a dissipation

	N	$\nu \times 10^4$	R_λ	E	ε	H	h	$\eta_\varepsilon \times 10^3$	$\eta_h \times 10^4$
I	512	1	270	1.72	1.51	-26.8	62.2	1.7	9
II	1024	0.35	430	1.87	1.75	-0.12	13.2	1.3	4

TABLE I: Parameters of the numerical simulations I and II. ν - viscosity; R_λ - Taylor Reynolds number; mean total energy $E = \frac{1}{2} \sum_k \tilde{\mathbf{u}}(\mathbf{k})^2$; ε - mean energy dissipation rate; mean total helicity $H = \sum_k \tilde{\mathbf{u}}(\mathbf{k}) \cdot \tilde{\boldsymbol{\omega}}(-\mathbf{k})$; h - mean helicity dissipation rate; $\eta_\varepsilon = (\nu^3/\varepsilon)^{1/4}$; $\eta_h = (\nu^3/h)^{1/5}$.

scale which is larger than the Kolmogorov dissipation scale, suggesting that the joint cascade is truncated sooner if helicity is present.

We performed two simulations of the three-dimensional (3- d), forced Navier-Stokes equation in a unit-periodic box with 512 (data I), and 1024 (data II) grid points to a side respectively. In these units, the wavenumber k is in integer multiples of 2π . Energy and helicity were injected into the flow for $k \leq 2$ at each time-step. The forcing scheme was the same as in [8]. For case I we imposed maximum helicity in $k \leq 2$ [4, 9]. For case II the helicity input was uncontrolled and random, resulting in a small but finite mean helicity over the time. The spectra for case I were averaged over 40 snapshots spanning 8 large-eddy turnover times after spin-up. The spectra for case II were averaged over 48 snapshots spanning 2 large-eddy turnover times after spin-up. The spin-up time in each case was defined to be when the input rate of energy matched the dissipation rate of energy. Additional parameters of the simulations are given in Table I.

Following the argument in [5] for the derivation of τ_E , we define the time-scale τ_H for transfer based on the antisymmetric co-spectrum,

$$\tau_H^2 \sim \left(\int_0^k |\tilde{E}(p)| p^2 dp \right)^{-1} \sim \left(\frac{1}{2} |H(k)| k^2 \right)^{-1}. \quad (3)$$

The distortion corresponding to τ_H is different from the distortion corresponding to τ_E . The shear in the former case corresponds to a 'twist', an out-of-plane motion for which the time-scale is different than the in-plane shear rate corresponding to τ_E .

We estimate the transfer rate (flux) of helicity through wavenumber k , $F_H(k) \sim kH(k)/\tau_H \sim kH(k)(H(k)^{1/2}k)$. Assuming steady-state, inertial range behavior with constant flux of helicity $F_H(k) = h$, the mean helicity dissipation rate, we obtain

$$H(k) \approx h^{2/3} k^{-4/3}. \quad (4)$$

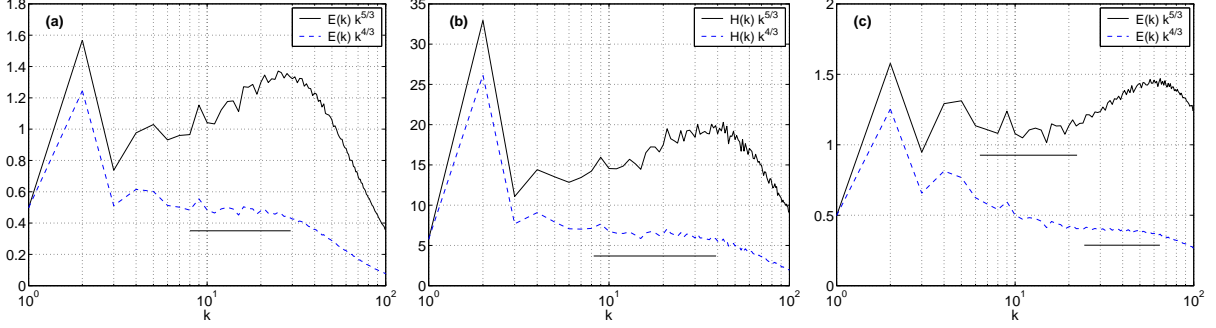


FIG. 1: Compensated spectra of (a) energy and (b) helicity, for data I. Observe the $k^{-4/3}$ scaling (dashed curve) range indicated by the horizontal line segment. (c) Compensated energy spectrum for data II. The horizontal line segments indicate ranges of $k^{-5/3}$ (solid curve) and $k^{-4/3}$ (dashed curve) scaling.

We compare τ_H with the Kraichnan time-scale for energy transfer $\tau_E^2 \sim (E(k)k^3)^{-1}$ [5],

$$\frac{\tau_E}{\tau_H} \sim \left(\frac{|H(k)|}{2kE(k)} \right)^{1/2}. \quad (5)$$

Since $[|H(k)|/(2kE(k))]^{1/2} \gg |H(k)|/(2kE(k))$ as the latter tends to zero, Eq. (5) implies that even for small values of the relative helicity, the time-scales can become comparable. We can then justifiably ask what the effect of τ_H will be on the energy spectrum. The energy flux ε through wavenumber k is

$$\varepsilon \sim \frac{kE(k)}{\tau_H} \sim kE(k)H(k)^{1/2}k. \quad (6)$$

Using Eq. (4) in Eq. (6), we get

$$E(k) \approx \varepsilon h^{-1/3} k^{-4/3}. \quad (7)$$

To summarize thus far, the τ_E dynamics result in Kolmogorov $k^{-5/3}$ scaling in both energy and helicity spectra, whereas τ_H dynamics result in $k^{-4/3}$ scaling in both. Clearly, the steeper $k^{-5/3}$ scaling should dominate in the low-wavenumbers while the $k^{-4/3}$ should manifest in the higher wavenumbers. In order for the latter scaling to be visible in the high wavenumbers, however, τ_H must still be comparable to τ_E . According to Eq. (5), this may occur for rather modest relative helicity in the high wavenumbers, contrary to previous assumptions. The main point of our Letter is that in general, the helicity timescale τ_H may not be ignored.

Figure 1 shows the energy and helicity spectra from our simulations. Each of the spectra are compensated by $k^{4/3}$ and by $k^{5/3}$ in order to distinguish the dominant scaling. For the strongly helical case I, there is good agreement with $k^{-4/3}$ scaling for both the energy and helicity spectra in approximately the same range (Figures 1(a) and (b)). Note that the compensation with $k^{5/3}$ results in the commonly observed ‘bottleneck’ phenomenon which we will discuss below. The energy spectrum of II (Fig. 1(c)) shows a range of $k^{-5/3}$ scaling followed by a range of $k^{-4/3}$ scaling (which appears as a bottleneck in the $k^{-5/3}$ compensated plot). The relative helicities in the range $10 < k < 100$, where the $k^{-4/3}$ scaling is seen, are shown in Fig. 2. For I, the relative helicity falls from about 10% to about 3% corresponding to τ_E/τ_H ranging from 32% to 17% according to Eq. (5). Despite the small total helicity $H = -0.12$ of II, and its noisy helicity spectrum, its relative helicity values lie between 1% and 5%. This implies that τ_E/τ_H could be as much as 22%. In both cases τ_H is not much longer than τ_E . This is the first evidence of $k^{-4/3}$ scaling ranges in both energy and helicity spectra simultaneously. The possibility of a ‘pure’ or ‘maximal’ forward cascade of helicity scaling as $k^{-4/3}$ [3], with inverse cascade of energy scaling as $k^{-7/3}$ does not arise. This is because in our analysis we have retained the effect of the helical time-scale τ_H and allowed it to modify the spectral dynamics. Since the scaling corresponding to τ_H is $k^{-4/3}$, a slower decay than $k^{-5/3}$, its ‘signature’ in the spectra can dominate at large k even as the overall parity is being restored.

Based on the analysis above, we propose that the bottleneck in the total energy spectrum is in fact a *change in the scaling* of the energy spectrum, from a $k^{-5/3}$ regime in which the τ_E dynamics dominate to a less steep $k^{-4/3}$ regime in which the τ_H dynamics become significant. We will use the kinematic arguments of [10] with our new phenomenology and dynamics to analyse the bottleneck for such a helical influence. In simulations, it is possible to compute the total energy spectrum $E(k) = (1/2) \sum_{|\mathbf{k}|=k} |\tilde{\mathbf{u}}(\mathbf{k})|^2$ as a sum over a shell of radius k rather accurately. In experiments it is convenient to measure the one-dimensional (1- d) longitudinal and transverse spectra are computed along the measurement direction, say z . In our 3- d flow simulation we calculate the 1- d spectra as follows. The 1- d fourier transform in the z -direction of the velocity $\mathbf{u}(\mathbf{x})$ is $\tilde{\mathbf{u}}(x, y, k_z) = (1/N) \sum_{n=1}^N e^{ik_z z_n} \mathbf{u}(x, y, z_n)$ where $0 \leq k_z \leq \pi/\delta z$. The longitudinal (transverse) 1- d spectrum, averaged over the x - y plane, is

defined by

$$E_{L(T)}(k_z) = \frac{1}{(2N^2)} \sum_{p,q=1}^N |\tilde{u}_{z(\perp)}(x_p, y_q, k_z)|^2, \quad (8)$$

where $|\tilde{u}_{\perp}|^2 = |\tilde{u}_x|^2 + |\tilde{u}_y|^2$. In isotropic flow, the 1- d spectra should be independent of the direction in which the fourier transform is performed. Our time-averaged longitudinal spectra computed in the the x , y and z directions all collapse and the transverse spectra do the same. We average the 1- d spectra in the three coordinate directions and drop the use of the subscript z to denote the direction of the fourier transform. In isotropic flow there is a relation between the 1- d and 3- d spectra [10, 11],

$$E(k) = -k \left(\frac{dE_L}{dk} + 2 \frac{dE_T}{dk} \right). \quad (9)$$

Our spectra satisfy Eq. (9) very well for $k \geq 10$ and fairly well in the lower wavenumbers. As emphasized in [10], Eq. (9) is a local relationship, wherein the functional form of the total spectrum $E(k)$ is fully determined by the local behavior of E_L and E_T at a given wave number. For homogeneous, isotropic flows with helicity, it is reasonable to suppose that $E_L(k)$ (see definition in Eq. (8)) would mainly carry contributions from the in-plane shear time-scale τ_E . However $E_T(k)$, which is related to the transverse components of the velocity fourier transform, could be influenced by τ_H dynamics coming from $\tilde{E}(k)$. The correlation time between transverse components can be slowed down by the dynamics of $\tilde{E}(k)$ which arise due to the presence of helicity. Such coupling may not be deduced from kinematic arguments, it requires proper consideration of the new dynamics. Furthermore, it is not possible to see this coupling in the unclosed lowest-order Kármán-Howarth dynamical equations wherein the symmetric and antisymmetric parts completely decouple for homogeneous flows [7]. It was pointed out in [6] that higher-order statistical equations for helical turbulence should show the coupling. The coupling is seen explicitly in the EDQNM closure [12].

Figure 3 shows the compensated longitudinal and transverse spectra for simulation II. The bottleneck is greatly diminished in $E_L(k)$ (Fig. 3(a), solid curve) which shows close to $k^{-5/3}$ scaling throughout the inertial range. In $E_T(k)$ (Fig. 3(b), solid curve), the bottleneck persists although its peak occurs slightly earlier in wavenumber than the bottleneck for the corresponding total spectrum. For completeness, we have also shown the 1- d spectra compensated by $k^{4/3}$ (Fig. 3, dotted curves). Based on our arguments above, we might have expected a stronger $k^{-4/3}$ scaling region of the transverse spectrum; such behavior is not

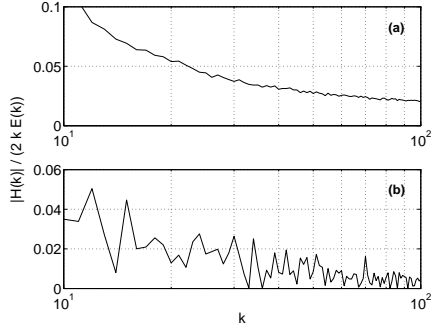


FIG. 2: The relative helicities for (a) data I and (b) data II, in the range $10 < k < 100$, where Fig. 1 shows $k^{-4/3}$ scaling. The relative helicity lies between 3% and 10% in (a) and between 1% and 5% in (b).

clearly observed although there appears to be a tendency towards a scaling much shallower than $k^{-5/3}$ and steeper than $k^{-4/3}$ in the bottleneck regime. We hope that our initial investigation provides motivation for further analysis of the bottleneck in transverse *vs.* longitudinal spectra. Our prediction is that the bottleneck will be stronger in the transverse spectrum than in the longitudinal one because of the greater contamination of the former by the helical co-spectrum dynamics. This raises the intriguing possibility that τ_H affects the scaling of transverse structure functions, accounting for some of the observed difference between the scaling exponents of longitudinal and transverse structure functions in near-isotropic, high-Reynolds number turbulence data [13]. Such contributions would appear as a parity-breaking in the *isotropic* small-scales, and might not be easily disentangled by, for example, the SO(3) group decomposition methods (see [14] and references therein) used to extract isotropic contributions to non-helical turbulence statistics.

We finally present a key result from analysis of the convergence of the dissipation integrals for a two-timescale cascade. In [4] the same analysis was performed assuming a single timescale τ_E . The total dissipation of energy and helicity may be written as $D_E = 2\nu(\int_0^{k_c} dk k^2 E(k) + \int_{k_c}^{k_d} dk k^2 E(k))$ and $D_H = 2\nu(\int_0^{k_c} dk k^2 H(k) + \int_{k_c}^{k_d} dk k^2 H(k))$, where

$$E(k) = \begin{cases} C_E \varepsilon^{2/3} k^{-5/3} & \text{for } k < k_c; \\ C_H \varepsilon h^{-1/3} k^{-4/3} & \text{for } k_c < k < k_d, \end{cases} \quad (10)$$

$$H(k) = \begin{cases} c_E \varepsilon^{-1/3} k^{-5/3} & \text{for } k < k_c; \\ c_H h^{2/3} k^{-4/3} & \text{for } k_c < k < k_d, \end{cases}, \quad (11)$$

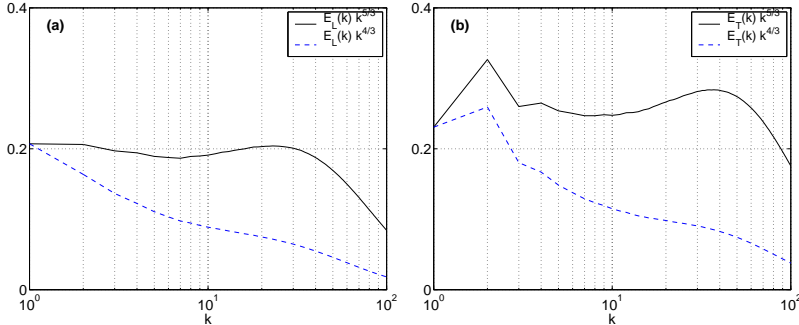


FIG. 3: Compensated (a) longitudinal and (b) transverse energy spectra for the simulation II. $E_L(k)$ shows a diminished bottleneck where the full spectrum $E(k)$ of Fig. 1(c) has a pronounced bottleneck. $E_T(k)$ shows a range of $k^{-5/3}$ coinciding with that of Fig 1(c) and a persistent bottleneck with a tendency to $k^{-4/3}$ scaling in the region of the bottleneck.

and C_E, C_H, c_E and c_H are constants. The precise estimate of the transition wavenumber k_c is unimportant to what follows. The upper wavenumber k_d denotes the maximum beyond which the cascade is completely suppressed by viscosity. We obtain $D_E \sim \nu \varepsilon h^{-1/3} k_d^{5/3}$; $D_H \sim \nu h^{2/3} k_d^{5/3}$. In [4] $k_d = k_\varepsilon \sim (\varepsilon/\nu^3)^{1/4}$ (the Kolmogorov dissipation wavenumber). In our case, setting $k_d = k_\varepsilon$ causes the integrals to diverge as $\nu^{-1/4}$ in the limit $\nu \rightarrow 0$. The choice $k_d \sim (h/\nu^3)^{1/5}$ ensures that the integrals converge to their correct values for statistically steady-state, $D_E = \varepsilon$ and $D_H = h$. We will call this new wavenumber k_h since it depends solely on the helicity dissipation rate. It must be distinguished from the k_H of [15] which depends on both energy and helicity dissipation rates. In the limit $\nu \rightarrow 0$, $k_\varepsilon \gg k_h$. In our simulations $k_\varepsilon > k_h$ by a factor of about 2.5. While in agreement with our analysis, we cannot really distinguish between the two wavenumbers in this data. However, we suggest that the resolution requirements for measurements in turbulence with helicity might be weaker than those in turbulence without helicity.

We thank U. Frisch for useful discussions and for bringing our attention to Ref. [10]. Part of this work was completed during the visit of two of the authors (SK and TM) at the Observatoire de la Côte d’Azur, Nice, France.

[1] J. J. Moreau, C. R. Acad. Sci. Paris **2522810**, 2810 (1961).

[2] H. K. Moffat, J. Fluid Mech. **35**, 117 (1969).

- [3] A. Brissaud, U. Frisch, J. Leorat, M. Lesieur, and A. Mazure, *Phys. Fluids* **16**, 1366 (1973).
- [4] Q. Chen, S. Chen, and G. L. Eyink, *Phys. Fluids* **15**, 361 (2003).
- [5] R. H. Kraichnan, *J. Fluid Mech.* **47**, 525 (1971).
- [6] R. Betchov, *Phys. Fluids* **4**, 925 (1961).
- [7] S. Kurien, *Physica D* **175**, 167 (2003).
- [8] M. Taylor, S. Kurien, and G. L. Eyink, *Phys. Rev. E* **68**, 026310 (2003).
- [9] W. Polifke and L. Shtilman, *Phys. Fluids A* **1**, 2025 (1989).
- [10] W. Dobler, N. E. L. Haugen, T. Yousef, and A. Brandenburg, *Phys. Rev. E* **68**, 026304 (2003).
- [11] A. S. Monin and A. Yaglom, *Statistical Fluid Mechanics*, vol. 2 (MIT Press, Cambridge, MA, 1987).
- [12] J. Andre and M. Lesieur, *J. Fluid Mech.* **81**, 187 (1977).
- [13] K. R. Sreenivasan and B. Dhruva, *Progr. Theoret. Phys. Suppl.* pp. 103–120 (1998), ISSN 0375-9687.
- [14] S. Kurien and K. R. Sreenivasan, in *New Trends in Turbulence*, edited by M. Lesieur, A. Yaglom, and F. David (Springer-Verlag, Berlin, 2001), Proceedings of the Les Houches Summer School 2000, p. 53.
- [15] P. D. Ditlevsen and P. Giuliani, *Phys. Fluids* **13**, 3508 (2001).